# Development of a Double-Oblique-Shock Scramjet Model in a Shock Tunnel

I. T. OSGERBY,* H. K. SMITHSON,* AND D. A. WAGNER†
*ARO Inc., Arnold Air Force Station, Tenn.*

**A double-oblique-shock Scramjet has been developed using the AEDC-VKF 16-in. Shock Tunnel I at a freestream Mach number of 11. The model was developed as a test bed for the development of instrumentation and hydrogen fuel injection techniques for supersonic combustion experiments to be conducted at the 54-in. test section in the AEDC-VKF Tunnel F. Difficulties were encountered, especially at the entrance to the combustor because of the combined action of separation and the interaction of the second shock from the cowl lip. Satisfactory, repeatable performance was obtained with a porous metal inlet ramp to remove the low momentum portion of the inlet boundary layer. The highest total pressure recovery in the combustor was obtained with the porous inlet ramp installed. The measured pressure levels were approximately 50% less than the values predicted for inviscid two-shock performance. The primary pressure losses were attributed to viscous-inviscid flow interactions at the combustor entrance and secondary pressure losses were due to source flow effects in the conical tunnel nozzle flow.**

## Nomenclature

| | |
|---|---|
| $A$ | = area |
| $ER$ | = equivalence ratio |
| $H$ | = total specific enthalpy |
| $L_0$ | = length of combustor for 95% complete reaction |
| $M$ | = Mach number |
| $p$ | = pressure |
| $\dot{q}_w$ | = heat-transfer rate per unit area to wall |
| $Re$ | = Reynolds number |
| $T$ | = temperature |
| $U$ | = flow velocity |
| $X$ | = distance from plate leading edge or combustor entrance |
| $\rho$ | = density |
| $\tau_{ID}$ | = ignition delay time |
| $\tau_R$ | = reaction time |

### *Subscripts*

| | |
|---|---|
| 0 | = reservoir (total) condition |
| $\infty$ | = freestream condition in tunnel test section |
| 2 (or $R$) | = conditions on the ramp inlet behind the first oblique shock |
| 3 (or $C$) | = conditions in the combustor behind the second oblique shock |
| $ex$ | = conditions at the exit plane of the combustor |
| $l$ | = laminar boundary layer |
| $t$ | = turbulent boundary layer |
| $w$ | = wall condition |
| $x$ | = denotes a local value |

### *Superscripts*

| | |
|---|---|
| $'$ | = value behind a normal shock |

## Introduction

A PROGRAM is underway to evaluate the feasibility of using Tunnel F [Gas Dynamic Wind Tunnel, Hypersonic (F)] of the von Kármán Gas Dynamics Facility (VKF)[1,2] for testing integrated Scramjet models. Tunnel F is an arc-heated hypervelocity (hotshot) wind tunnel with 108-in.-diam test section (Mach 14–22) and a 54-in. test section (Mach 10–18). A useful run time of between 50 and 200 msec is attained. In terms of Mach number and Reynolds number, a wide range of flight conditions is simulated, using nitrogen as the test gas. The results of a series of tunnel calibration tests using air as a test gas were reported in Ref. 3 It was demonstrated that clean (unvitiated) airflow could be generated at a stagnation temperature of 3000°K and stagnation pressures up to 10,000 psia. Current tunnel development programs (including an enlarged arc chamber) are aimed at increasing this capability to 4000°K stagnation temperature at 20,000-psia pressure, or 2000°K at 40,000 psia.

A concurrent program was initiated to develop the instrumentation and theoretical tools necessary to obtain and analyze data during a test of a Scramjet model in the tunnel. Such a program required a model with which the previous development could be carried out. The results reported here were obtained in this program. The development of the model entailed a good deal of experimental research, thus, the test program was conducted in the AEDC-VKF 16-in. shock Tunnel I.[4,5] The 54-in. test section of Tunnel F will be used in a subsequent test program.

The development of the model and results of aerodynamic performance tests are presented. The results of combustion tests, using this model, will be published in a subsequent report.

## Experimental Equipment and Test Conditions

The shock tunnel[4,5] is operated in the tailored-interface mode at a primary shock Mach number of 3.83. The air is expanded through a 5° half-angle conical nozzle to a velocity of about 6700 fps (freestream Mach number 11). The reservior conditions and the resulting test section flow properties are summarized in Table 1. The gas properties were computed using equilibrium thermodynamic properties of air.[6–8]

### Double-Oblique-Shock Model

It was recognized that a double-oblique-shock inlet was an impractical device for efficient or even realistic total pressure recovery for a Scramjet; however, the object of the test pro-

Received February 4, 1970; revision received July 24, 1970. The work reported herein was supported by the Arnold Engineering Development Center, Air Force Systems Command, under Contract F40600-69-C-0001 with ARO Inc. Further reproduction is authorized to satisfy needs of the U. S. Government.

* Project Engineer, von Kármán Facility, Hypervelocity Branch. Member AIAA.

† Project Engineer, von Kármán Facility, Hypervelocity Branch. Associate Member AIAA.

**Table 1 Typical run conditions**

| | |
|---|---|
| Reservoir conditions | |
| Reflected shock pressure, $p_{5s}$ | 708 atm |
| Reflected shock temperature, $T_{5s}$ | 1860°K |
| Freestream conditions | |
| Pressure, $p_\infty$ | 0.00817 atm (0.12 psia) |
| Temperature, $T_\infty$ | 88°K |
| Velocity, $U_\infty$ | 6789 fps |
| Reynolds number, $Re_\infty$/ft | $3.38 \times 10^6$ |
| Mach number, $M_\infty$ | 11 |

gram was to develop a simple model in which supersonic combustion could be demonstrated and used for instrumentation development. Calculations (assuming inviscid flow) indicated that flow deflection angles of 25° should generate a compatible combination of static pressure, temperature, and Mach number in the combustor which should be adequate for spontaneous combustion of hydrogen as shown in Table 2. Estimates of the ignition and reaction time were obtained from Ref. 9.

The model is shown installed in Tunnel I in Fig. 1. It is desirable for the shock from the leading edge of the upper combustor plate (cowl) to impinge on the ramp-combustor intersection so that the Prandtl-Meyer expansion fan is cancelled by the shock wave. For this case the ramp angle, ramp length, and the freestream Mach number determine the position of the leading edge of the upper combustor plate and the channel height.

The model was fabricated with an inclined flat plate ramp section 3 in. wide and 7 in. long. These dimensions were a compromise based on obtaining a suitable combustor channel height (controlled by ramp length) for optical measurements but sacrificing plate width to prevent tunnel flow blockage. A combustor length of 5 in. was chosen which allowed the whole model to remain within the field of view of the schlieren system (the width is the same as for the inlet).

The sidewall windows were of schlieren quality quartz, 0.25 in. thick, mounted in a steel frame. The position of the windows could be adjusted longitudinally. With side windows attached, the combustor channel height was limited to nominal values of 0.3 and 0.5 in.

## Instrumentation

Heat-transfer measurements were made with slug calorimeters. The calorimeter consists of a thin-film platinum resistance thermometer deposited on an anodized aluminum disk. Wall static pressures were measured with gage diaphragm pressure transducers. This type of pressure transducer consists of a semiconductor strain gage mounted directly on a thin metal diaphragm. Pitot pressures were measured with quartz piezo gages.

Typical reservior, test section Pitot, and model combustor exit Pitot traces are shown in Fig. 2. Test data were taken during the period of constant Pitot pressure. The upper trace corresponds to the reservoir (total) pressure (reflected shock region pressure). The middle trace corresponds to the freestream Pitot (stagnation) pressure as measured by the Pitot

**Table 2 Model design conditions two-shock theory (inviscid)**

| | Freestream | Ramp | Combustor |
|---|---|---|---|
| $p$, psia | 0.12 | 4.8 | 27.3 |
| $T$, °K | 88 | 647 | 1160 |
| $M$ | 11.0 | 3.5 | 2.1 |
| $U$, fps | 6789 | 5819 | 4635 |
| $\tau_{id}$, $\mu$sec | ... | ... | 17 |
| $\tau_R$, $\mu$sec | ... | ... | 10 |
| $L_0$, in. | ... | ... | 1.50 |

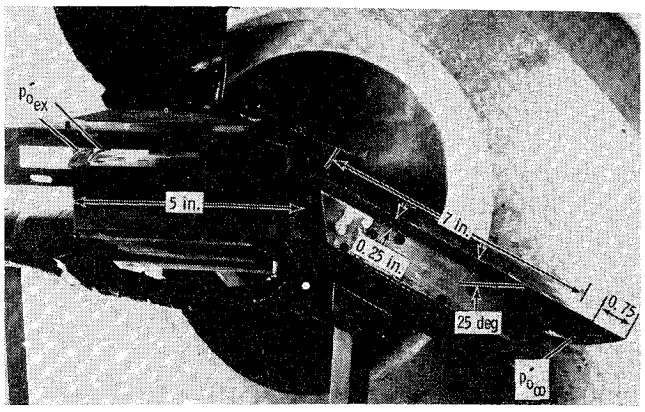


**Fig. 1 Model installed in Tunnel I.**

gage ($p_{0_\infty}'$) as shown on the side of the inlet in Fig. 1. It is shown that the tunnel achieves a uniform condition approximately 1 msec after the initial starting shock arrives, and the Pitot pressure remains relatively constant for 2 or 3 msec. The bottom trace corresponds to the Pitot pressure measured at the exit plane of the combustor. The combustor exit Pitot gages may be seen through the sidewalls in Fig. 1. The start time of the combustor can be seen to be about the same as for the tunnel since the Pitot pressure at the combustor exit achieves a relatively constant pressure about 1 msec after the beginning of the pressure rise.

## Experimental Results

### Static Pressures and Heat-Transfer Rates on the Flat Plate Ramp

Static pressure and surface heat-transfer rates on the flat plate ramp at an angle of attack of 25° are shown in Fig. 3.

The decay of static pressure along the ramp is the result of the combined effects of source flow and edge losses.

#### *Source Flow Effects*[10]

The nozzle consists of a throat section with an exit radius of curvature that matches the slope of the 5° half-angle conical nozzle. The nozzle flow, therefore, continues to expand in the test section, giving rise to gradients in the fluid-dynamic and state variables. An additional complication is introduced for a flat plate at angle of attack since the inclination of the plate to the freestream velocity vector varies along the plate length. The variation in static pressure along the flat plate at angle of attack attributable to source flow is shown in Fig. 3. The results are in good agreement; however, only centerline pressures were measured. Additional pressure losses can be expected due to edge losses.

#### *Edge Effects*

The pressure on the surface of the plate at angle of attack is higher than the freestream pressure. Thus, without sidewalls, the gas is free to expand from the ramp, spilling over the sides. Since the gas flow on the plate is supersonic, a region of quasi-one-dimensional flow exists, having a bound-

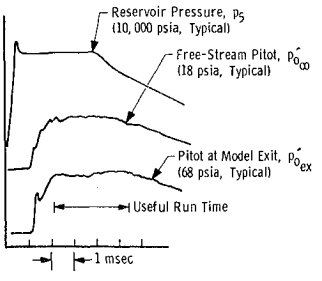


**Fig. 2 Typical pressure traces.**

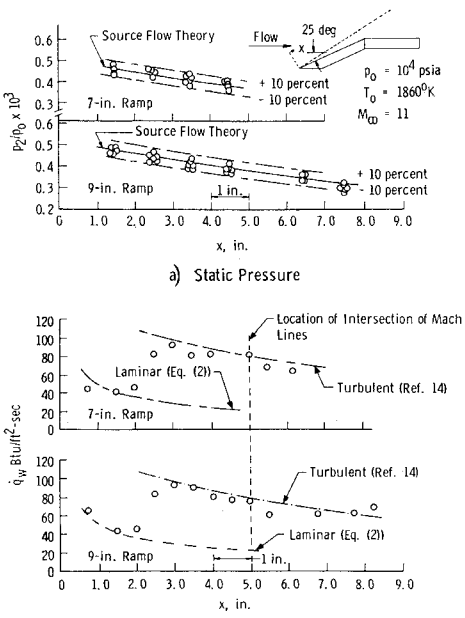


**Fig. 3 Static pressure and heat-transfer rates on the flat plate ramp at 25°.**

ary confined by the local Mach lines drawn from the tips of the plate. Only source flow effects should be evident in data taken within the boundary.

The heat-transfer rate distributions shown in Fig. 3 indicate that the end of transition from a laminar to a turbulent boundary layer occurs about 3 in. from the leading edge of the plate. Based on current transition literature, the end of transition was expected to occur at approximately 6 or 7 in. The edge effect induced cross flows in the boundary layer on the plate that may have contributed to the early transition. Theoretical estimates of turbulent heat-transfer rates were

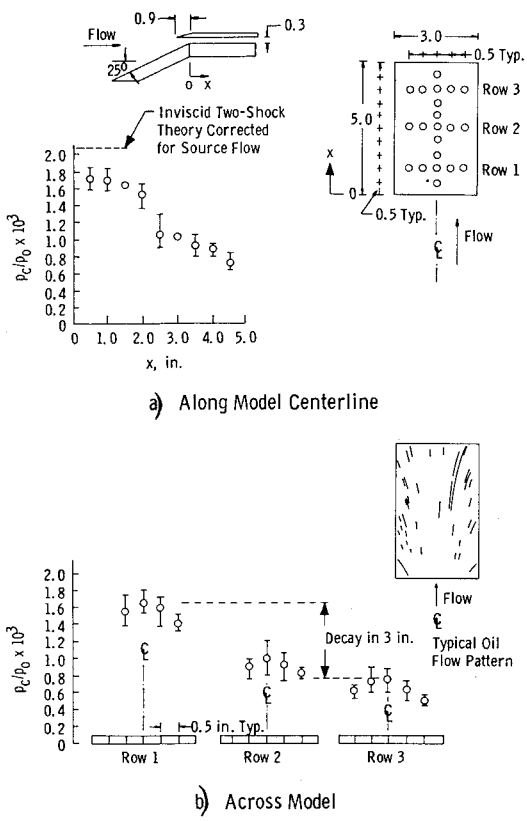


**Fig. 4 Combustor section pressure distribution (model without sidewalls).**

obtained by the method of Arthur.[11] No account of the axial pressure gradient was included in the estimates.

Theoretical values of laminar heat transfer are given by‡:

$$\dot{q}_{wl} \approx 0.332\rho_\infty U_\infty(H_0 - H_w)[Re_{\infty x}]^{1/2}[p_2/p_\infty]^{1/2} \quad (1)$$

where $Re_{\infty x}$ is a Reynolds number per unit length based on freestream conditions, and $\dot{q}_{wl}$ is the laminar heat-transfer rate (Btu/ft²-sec). The derivation of this equation is given in Ref. 12.

Different ramp lengths on the model were used to determine whether tunnel blockage effects were present in the data shown in Fig. 3. Comparison of the data from ramp lengths of 7 and 9 in. indicates that tunnel blockage was not a significant factor.

### Model without Sidewalls

Static pressures measured in the combustor section with the sidewalls removed are shown in Fig. 4. Again, a pressure decay (parallel to the model centerline in Fig. 4a and perpendicular in Fig. 4b) was obtained because of mass flow loss from the open sides of the combustor. Oil droplet flow patterns (also shown in Fig. 4) taken during some of the tests confirmed that considerable outflow occurred both from the ramp and combustor. Thus, the flow was not one-dimensional, and significant lateral gradients in fluid dynamic and state variables existed.

### Model with Sidewalls

Sidewalls were installed on the model to reduce the mass flow losses in the combustor. The initial configuration tested is shown in Fig. 5a. The combustor channel height was approximately 0.3 in., and the leading edge of the sidewall windows was placed at the leading edge of the upper combustor plate. The model did not start during the useful run time of approximately 2–3 msec, and the static pressures did not

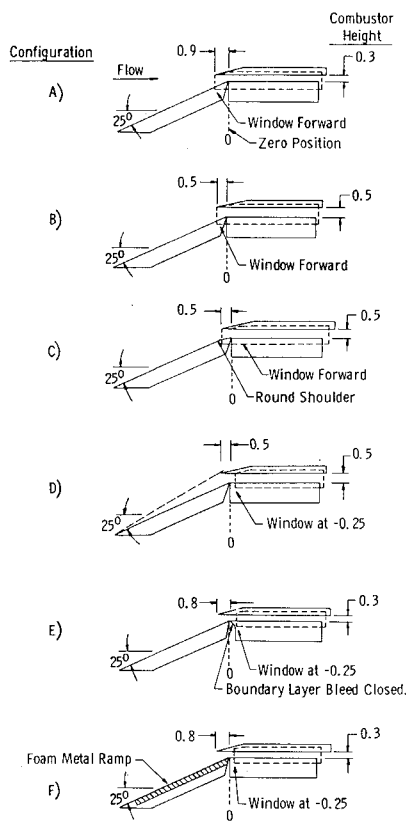


**Fig. 5 Model configurations (with sidewalls).**

‡ This correlation was suggested by J. D. Whitfield, ARO Inc., Chief of the von Kármán Gas Dynamics Facility, Arnold Engineering Development Center.

achieve a uniform level. Schlieren motion pictures showed that the inlet boundary layer was separated and that a normal shock was standing at the combustor entrance. A number of variations in model configuration were investigated in an attempt to establish uniform, supersonic flow in the combustor. These tests are described below.

### *Effects of Increasing the Combustor Channel Height*

The combustor channel height was increased from 0.3 to 0.5 in. to increase the ratio of inviscid flow height to boundary-layer thickness. In addition, the upper combustor plate (cowl) was moved back in order to maintain shock on cowl lip operation as shown in Fig. 5b. Steady, supersonic flow was established with this model configuration, and results are shown in Fig. 6a (square symbols). Comparison with the pressure ratio results in Fig. 4a obtained with the model without sidewalls shows that 1) the pressure ratio near the entrance of the combustor was reduced from 0.0017 to 0.0008 with the model with sidewalls; and 2) the pressure ratio near the exit of the combustor was increased from 0.0007 to 0.0010.

The pressure ratio predicted by inviscid, two-shock theory is 0.00275, which is reduced by source flow effects to approximately 0.0020. Obviously, additional pressure losses of considerable magnitude were present. The primary pressure loss mechanisms are spillage and the effect of the boundary layer generated on the inlet modifying the interaction of the second shock from the cowl lip and the Prandtl-Meyer expansion fan at the sharp corner junction of the inlet and combustor. Based on inviscid, two-shock theory, the second shock must impinge exactly on the corner to cancel the Prandtl-Meyer expansion fan. When the combustor height was increased, it was necessary to move the upper combustor plate back, thus the second shock impinged behind the corner, downstream of the expansion fan. When a round shoulder was used, as shown in Fig. 5c, more of the flow was expanded before seeing the second shock, and an additional pressure loss was observed as shown in Fig. 6a (circular symbols). A secondary pressure loss mechanism is the interaction of the shock waves generated by the leading edge of the windows with the combustor entrance flowfield. Results of tests with a combustor height of 0.5 in. and windows retracted to a position behind the junction of the inlet and combustor (as in configuration 5d) are shown as circles in Fig. 6b. Comparison of the Pitot pressures—measured at the combustor exit plane—in Figs. 6a and 6b shows that the total pressure losses in the model flowfield were significantly reduced with the

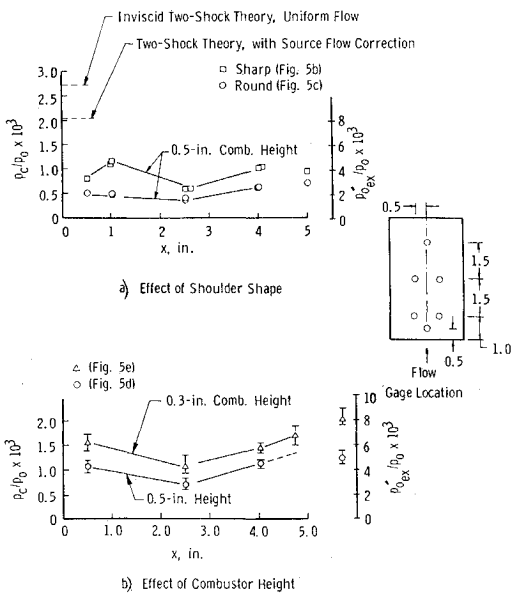


**Fig. 6 Effect of shoulder shape and combustor height on combustor pressure.**

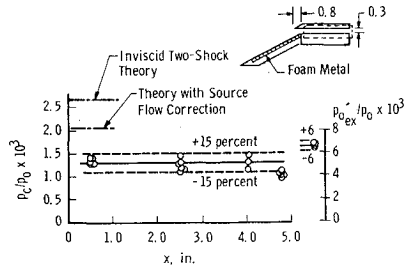


**Fig. 7 Effect of porous inlet ramp on combustion section pressure.**

windows retracted. Since a significant increase in the ratio of Pitot pressure from 0.004 to 0.005 was obtained by retracting the window position, it was decided to reduce the combustor height to approximately 0.3 in. again in order to move the second shock back to the corner. The results of tests with this configuration (identical to Fig. 5e, with the boundary-layer bleed closed) are shown as triangles in Fig. 6b. Comparison of the Pitot pressure ratios in Fig. 6b shows that a dramatic improvement in total pressure recovery was obtained. An increase in static pressure ratio from 0.0010 to 0.0015 was also obtained; however, even this value is substantially lower than the source flow corrected inviscid value of 0.002. Additional tests with the window leading edge forward of the position shown in Figs. 5d–f led to additional pressure losses and the station $X = -0.25$ in. was used in all subsequent tests.

It was apparent that most of the pressure losses were attributable to shock/boundary-layer interactions; thus, some tests were conducted to determine whether removal of all or part of the ramp boundary layer would improve the model pressure recovery.

### *Ramp Boundary-Layer Control*

A boundary-layer bleed was placed at the ramp combustor section corner as shown in Fig. 5e. The width of the bleed slot was varied from 0.020 to 0.080 in. The boundary-layer bleed had no significant effect on the model performance. Apparently the boundary layer was already separated before reaching the bleed.

The porous metal ramp (Figs. 1 and 5f) was found to be quite effective in controlling the ramp boundary layer. Measured static and exit Pitot pressures for the foam metal ramp are shown in Fig. 7. The static pressure distribution was more uniform than for previous configurations. The Pitot pressures were more consistent and repeatable.

Schlieren motion pictures showed that the separation shock at the intersection of ramp and combustor was much weaker in the tests with the foam metal ramp model. The 60% dense foam metal provides continuous boundary-layer suction, utilizing the pressure differential between the ramp surface and the evacuated interior of the model. It was estimated that 0.5% of the ramp mass flow was removed through the porous ramp. The improvement in inlet pressure recovery was attributed to the fact that the low momentum portion of the boundary layer was removed, which improves the stability of a boundary layer.

## Discussion and Summary of Experimental Results

The effects of the various changes in model configuration on the combustor exit Pitot pressure and Mach number are summarized in Fig. 8. The highest Pitot pressure recovery was obtained with a combustor height of 0.3 in. for which the second shock impinged close to the sharp corner. This corresponds to the most effective cancellation of the Prandtl-Meyer expansion fan by the compression shock. Complete cancellation could not be obtained primarily because of the boundary layer and secondarily because of mechanical diffi-

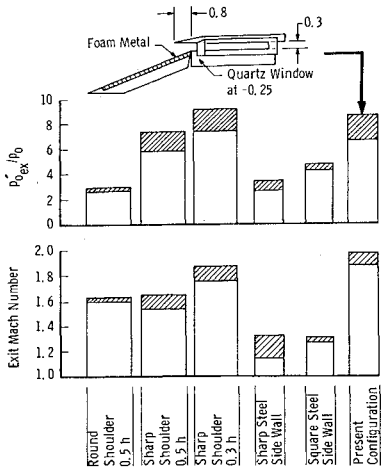


**Fig. 8 Pitot pressures and Mach numbers for various configurations.**

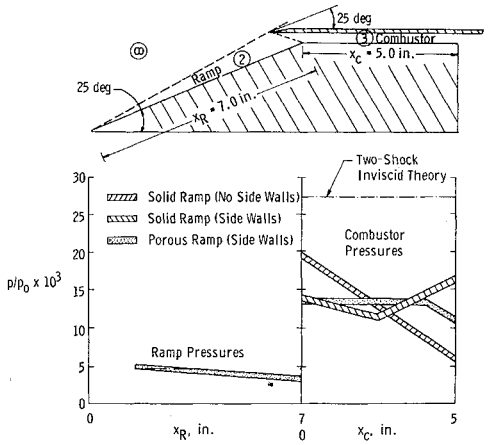


**Fig. 9 Summary of static pressure in the combustor.**

culties in assembly and alignment. Of the configurations having the highest pressure recovery, the porous ramp was the better of the two because of the more uniform static pressure in the combustor as shown in Fig. 9. Also shown in Fig. 9 are the ramp pressures, two-shock theory level, and the open sidewall model data to show the marked improvement in over-all model performance. The uniform level of the static pressures in the combustor with the porous ramp model should make interpretation of the pressure data for tests with injection easier than with the other configurations.

The data in Fig. 9 illustrate that although an improvement in pressure level and uniformity has been obtained, there is approximately a 50% difference in the inviscid two-shock theory level and the experimental values from tests with the porous ramp model. This difference could be caused by a number of factors, among them the following: 1) three-dimensional flow effects caused by the low aspect ratio of the ramp (edge losses) and by tunnel source flow; 2) viscous effects (boundary-layer displacement and momentum losses); 3) Oblique-shock-boundary-layer interactions; and 4) the complex interaction between the inviscid and viscous flowfield at the intersection of the ramp and combustor.

The pressure decay caused by source flow effects on the ramp accounts for a drop of static and Pitot pressure level in the combustor of approximately 22 and 15%, respectively.

Investigation of schlieren motion pictures indicated that relatively weak shocks were present in the combustor flow. Thus, the primary pressure loss mechanism is though to be caused by interactions at the combustor entrance.

The static and hence Pitot pressures are apparently strongly influenced by the abrupt exit expansion at the combustor exit as shown by the decrease in pressure ratios (Fig. 9). The measured values at the exit are approximately $p_3 \approx 11$ psia and $p_0'_3 \approx 68$ psia, and the estimated corresponding total pressure is $p_{0,3} \approx 107$ psia (assuming $\gamma \approx 1.3$). The average measured value of static pressure in the combustor is $\approx$13.5 psia. Assuming the flow near the combustor exit undergoes an isentropic expansion from 13.5 to 11 psia, which increases the flow Mach number (the expansion could be caused by a decrease in boundary-layer thickness, because of a base pressure effect, and hence an increase in inviscid flow area), the average Pitot pressure in the combustor is $p_0'_3 \approx 74$ psia.

The estimated static temperature in the combustor is $\approx$1200°K, using Mollier data and assuming adiabatic flow (heat transfer to the model, based on experimental values of heat-transfer rate, is approximately 5% of the total enthalpy, thus, the assumption of adiabatic flow is realistic).

## Combustion Considerations

The estimated ignition delay and reaction times[9] for an average static pressure and temperature of 13.5 psia and 1200°K are, respectively,

$$\left.\begin{aligned} \tau_{ID} &\approx 25\mu\text{sec} \\ \tau_R &\approx 27\mu\text{sec} \end{aligned}\right\} \text{fuel/air premixed}$$
$$\left.\begin{aligned} \tau_{ID} &\approx 25\mu\text{sec} \\ \tau_R &\approx 27\mu\text{sec} \end{aligned}\right\} \text{hydrogen fuel}$$

Thus, the time required for complete reaction is approximately double that estimated for two-shock theory performance shown in Table 2. In combustion experiments, the hydrogen fuel will not be premixed and will also be at 300°K, which will cool the air below 1200°K. For example, for an over-all equivalence ratio of 0.2, the mixture temperature will be 1130°K, resulting in $\tau_{ID} \approx 41.3$ $\mu$sec and $\tau_R \approx 29$ $\mu$sec; thus, the time required for complete combustion will then be approximately three times the two-shock theory estimate. This means that the length required for combustion of the fuel will be increased from 1.5 in. ($L_0$ in Table 2) to at least 4.5 in., with an additional length to be added for mixing of the fuel and air. The length of model combustor available for both mixing and combustion is $\approx$4 in. since 1 in. of combustor length is necessary for installation of the plenum chamber for the hydrogen injection.

It is obvious that the current performance is rather marginal for combustion testing, hence a heater will be installed on the driver tube of the shock tunnel to increase the total enthalpy and the static temperatures throughout the flowfield.

## Conclusions

1) A double-oblique-shock Scramjet has been developed with which it should be possible to do supersonic combustion tests. 2) The measured pressure levels (combustor Pitot and static) are approximately 50% less than the values predicted for inviscid two-shock performance. 3) The pressure losses (combustor Pitot and static) are attributed to two main causes. a) Source flow effects in the conical tunnel nozzle generate a decay in static pressure on the inclined flat plate inlet leading to a pressure level in the combustor approximately 22% below the two-shock theory level. b) Spillage at the combustor inlet and inviscid-viscous flow interactions between the boundary layer on the ramp, the second shock from the cowl lip, and Prandtl-Meyer expansion at the junction between the inlet and combustor are the major contributors to the additional reduction in pressure level in the combustor of approximately 28%. 4) The highest pressure recovery coupled with a uniform pressure distribution was obtained with a porous inlet ramp and a model configuration in which the shock from the cowl lip impinged closest to the junction of the inlet and combustor. This configuration allows the most effective cancellation of the Prandtl-Meyer expansion at the junction. 5) Combustion testing with this would lead to only partial combustion within the combustor because of the large static pressure losses, hence the total

enthalpy of the flow is to be increased by heating the shock tunnel driver section.

## References


[1] Ball, H. W., "Calibration of the 100-inch Hypervelocity Tunnel F," AEDC-TDR-63-46 (AD298279), March 1963, Arnold Engineering Development Center, Arnold Air Force Station, Tenn.

[2] Griffith, B. J. and Weddington, E. D., "Recent Refinements and Advancements of Hypersonic Testing Techniques in the 100-inch Tunnel F of the von Kármán Gas Dynamics Facility," *Proceedings of the Fourth Hypervelocity Techniques Symposium*, Arnold Engineering Development Center, Arnold Air Force Station, Tenn., Nov. 15–16, 1965.

[3] Osgerby, I. T. and Smithson, H. K., "Operation of AEDC-VKF 100-inch Hotshot Tunnel F with Air as a Test Gas and Application to SCRAMjet Testing," AEDC-TR-67-242 (AD-664906), Dec. 1967, Arnold Engineering Development Center, Arnold Air Force Station, Tenn.; also presented at the Fifth Hypervelocity Techniques Symposium, Univ. of Denver, Colo., March 1967.

[4] Ball, H. W., "Initial Operation of the Pilot Counterflow Test Unit (I)," AEDC-TR-65-132 (AD465893), July 1965, Arnold Engineering Development Center, Arnold Air Force Station, Tenn.

[5] Haun, J. H. and Ball, H. W., "Calibration of the Shock Tunnel Component of Counterflow Range (I) at Mach 7.5," AEDC-TR-66-64 (AD632816), May 1966, Arnold Engineering Development Center, Arnold Air Force Station, Tenn.

[6] Hilsenrath, J. and Klein, M., "Tables of Thermodynamic Properties of Air in Chemical Equilibrium Including Second Virial Corrections from 1500°K to 15,000°K," AEDC-TR-65-68 (AD612301), March 1965, Arnold Engineering Development Center, Arnold Air Force Station, Tenn.

[7] Grabau, M. and Brahinsky, H. S., "Thermodynamic Properties of Air from 300 to 6000°K and from 1 to 1000 Amagats," AEDC-TR-66-247 (AD646172), Jan. 1967, Arnold Engineering Development Center, Arnold Air Force Station, Tenn.

[8] Lewis, C. H. and Burgess, E. G., III, "Charts of Normal Shock Wave Properties in Imperfect Air," AEDC-TDR-64-43 (AD433958), March 1964, Arnold Engineering Development Center, Arnold Air Force Station, Tenn.

[9] Pergament, H. S., "A Theoretical Analysis of Non-Equilibrium Hydrogen-Air Reactions in Flow Systems," AIAA, Paper 63-113, White Oak, Md., 1963.

[10] Whitfield, J. D. and Norfleet, G. D., "Source Flow Effects in Conical Hypervelocity Nozzles," AEDC-TDR-62-116 (AD276124), June 1962, Arnold Engineering Development Center, Arnold Air Force Station, Tenn.

[11] Arthur, P. D. et al., "Flat Plate Turbulent Heat Transfer at Hypervelocities," *Journal of Spacecraft and Rockets*, Vol. 3, No. 10, Oct. 1966, pp. 1549–1551.

[12] Osgerby, I. T., Smithson, H. K., and Wagner, D. A., "Development of a Double-Oblique-Shock SCRAMjet Model in a Shock Tunnel," AEDC-TR-69-59, Aug. 1969, Arnold Engineering Development Center, Arnold Air Force Station, Tenn.


APRIL 1971 J. AIRCRAFT VOL. 8, NO. 4

# Transonic Flight and Wind-Tunnel Buffet Onset Investigation of the F-8D Aircraft

E. K. DAMSTROM* AND J. F. MAYES†
*LTV Aerospace Corporation, Dallas, Texas*

**Flight and wind-tunnel tests of the F-8D aircraft were conducted within Mach 0.72 to 0.92 to establish the proper interpretation of various wind-tunnel data in predicting flight buffet onset. The divergence of the root-mean-square wing bending moment fluctuation agreed best with the flight onset defined by $\pm 0.05g$ peak-to-peak fluctuation of normal acceleration at the center of gravity. Buffet onset trimmed lift coefficient was increased approximately 0.08 when $\pm 0.05g$ normal acceleration fluctuation at the pilot station, rather than center of gravity, was used to define flight onset. The flight test data analysis disclosed an interesting decrease of the predominant frequency of acceleration fluctuation with increasing trimmed lift coefficient during the maneuver. Analysis of flight data suggested that the $g$ level, as well as frequency and amplitude of $g$ fluctuation, should be considered if buffet intensity is to be related to pilot functional capability.**

## Nomenclature

$\bar{c}$ = wing mean geometric chord, excluding leading-edge chord extension (141.4 in., full scale)
$c.g._{flt}$ = flight center-of-gravity location, fraction of $\bar{c}$
$c.g._{wt}$ = wind-tunnel moment reference location, fraction of $\bar{c}$
$C_A$ = axial force coefficient, axial force/$(q_\infty S)$
$C_L$ = lift force coefficient, lift/$(q_\infty S)$
$C_m$ = pitching moment coefficient, pitching moment/$(q_\infty S\bar{c})$ (ref. about $0.286\bar{c}$)
$C_p$ = wing trailing-edge pressure coefficient, $(P - P_\infty)/(q_\infty S)$
$g$ = gravitational acceleration unit
$N_Y$ = lateral acceleration, $g$
$N_Z$ = normal acceleration, $g$
$P$ = wing trailing-edge static pressure, lb/ft²
$P_\infty$ = freestream static pressure, lb/ft²
$q_\infty$ = freestream dynamic pressure, lb/ft²
$RN/L$ = freestream unit Reynolds number, $ft^{-1}$
$S$ = reference area, wing area excluding leading-edge chord extension (375 ft², full scale)
$x/c$ = chordwise station measured from leading edge of wing, including leading-edge chord extension, fraction of chord
$y/(b/2)$ = spanwise station measured from plane of symmetry, fraction of semispan
$\alpha$ = angle of attack of fuselage, deg

Presented as Paper 70-341 at the AIAA Fighter Aircraft Conference, St. Louis, Mo., March 5–7, 1970; submitted April 6, 1970; revision received July 24, 1970. The authors wish to acknowledge the contribution of the wind-tunnel data by NASA and the valuable assistance of E. J. Ray of NASA and H. R. Barnard of LTV Aerospace Corporation.

* Engineering Specialist, External Aerodynamics Group, Vought Aeronautics. Member AIAA.

† Senior Engineer, External Aerodynamics Group, Vought Aeronautics. Member AIAA.